Biosensors and Bioelectronics 26 (2010) 1420–1424

Contents lists available at ScienceDirect

Biosensors and Bioelectronics

journal homepage: www.elsevier.com/locate/bios

Disposable biosensor based on immobilisation of glutamate oxidase on Pt nanoparticles modified Au nanowire array electrode

Mamun Jamal, Ju Xu, Kafil M. Razeeb*

Tyndall National Institute, University College Cork, Lee Maltings, Cork, Ireland

ARTICLE INFO

Article history:
Received 14 April 2010
Received in revised form 14 July 2010
Accepted 19 July 2010
Available online 27 July 2010

Keywords:
Disposable biosensor
Nanowire array electrode
Pt nanoparticle
H_2O_2
Glutamate oxidase

ABSTRACT

Novel electrochemical platform based on Pt nanoparticle modified ordered three-dimensional gold nanowire arrays (PtNP/NAEs) for the amperometric sensing of H_2O_2 and glutamate is developed. Pt nanoparticle (PtNP) is fabricated by electrodeposition onto the 3D nanowires and characterised using scanning electron microscopy (SEM) and cyclic voltammetry. The deposited nanoparticles have an average size of 20 nm. The PtNP/NAE shows a linear response of up to 20 mM for H_2O_2 detection with a sensitivity of 194.60 $\mu A\,mM^{-1}\,cm^{-2}$ at 20 °C. It can detect 1 μM (S/N = 3) of H_2O_2 at normal condition without using any enzyme or mediator. Analytical performance of this electrode is tested by immobilising glutamate oxidase (GlutOx) through cross-linking in the matrix of bovine serum albumin (BSA), Nafion and glutaraldehyde. At physiological pH, the biosensor showed the sensitivity of 10.76 $\mu A\,mM^{-1}\,cm^{-2}$, with a linear range of up to 0.8 mM.

1. Introduction

Glutamic acid is one of the 20 proteinogenic non-essential amino acid. Glutamate (anion of glutamic acid) is a useful marker for the diagnosis of myocardial and hepatic disease (Fonnum, 1984; Rietz and Guilbault, 1975). Glutamate is the major excitatory neurotransmitter in the central nervous system. Increasing level of glutamate in the cerebra spinal fluids generates neurological disorders, such as stroke, Alzheimer's, and Parkinson's disease (Olney and Farber, 1995; Symthies, 1999). It is also responsible in learning, memory, neurodevelopment, biomaterial sensitivity, and synaptic plasticity (Martin et al., 2000; Umar et al., 2008). Certain physiological problems such as aggressive behaviour, visual-task learning, morphine-induced muscular rigidity and retrograde amnesia are related with the amount of this amino acid in the body. Therefore, precise monitoring of glutamate level in the extra cellular space of brain tissue (50–350 μM) is essential to understand the role of glutamate in these disorders. Various methods have been developed for glutamate determination based mainly on chromatography (Swanepoel et al., 1996), fluorescence (Chapman and Zhou, 1999), spectrophotometry (Valero and Garcia-Carmona, 1998) and capillary electrophoresis (Tucci et al., 1998). These methods are time-consuming and require expensive instruments. In the last decade, the immobilization of glutamate oxidase (GlutOx) or dehydrogenase on electrodes for the design of amperometric biosensors has been an area of intense research. Because glutamate dehydrogenase sensors require the addition of NAD^+ as a cofactor, the majority of glutamate sensors are usually based on GlutOx, where the concentration of glutamate is measured by monitoring the formation of hydrogen peroxide from the GlutOx-catalyzed oxidation of L-glutamic acid (glutamate) by dioxygen.

$$\text{Glutamate} + O_2 + H_2O \xrightarrow{\text{GlutOx}} \text{2-Oxoglutarate} + NH_3 + H_2O_2$$
$$H_2O_2 \rightarrow 2H^+ + O_2 + 2e$$

Recently ALT biosensor (Jamal et al., 2009) has been developed, which is based on immobilisation of GlutOx on commercial Pt electrode. This sensor used ferrocene carboxylic acid as a mediator in the solution form and showed a sensitivity of glutamate detection of 1.43 $\mu A\,mM^{-1}$. However, very few works have been done afterwards on glutamate sensor to improve the sensitivity. From the application point of view, the final goal of the biosensor technology lies in designing high-performance sensors with appropriate characteristics such as sensitivity, selectivity, response time, linear range, stability and reproducibility. To determine them, the key factors are the strategy on electrode fabrication and enzyme immobilisation. The applications of 3D electrodes (Kang et al., 2008; Pang et al., 2009; Wen et al., 2009) are getting popular recently due to their large surface area, which ultimately improves the sensitivity. However, the distribution of enzymes in the random 3D matrices such as sol–gel matrix (Yang et al., 2006), random porous matrix (You et al., 2009) are usually not uniform, increase steric hindrance for the analytes, resulting in relatively low electron transfer efficiency. Moreover, in this situation, smaller percentage of immo-

* Corresponding author. Tel.: +353 21 4904078; fax: +353 21 4270271.
E-mail address: kafil.mahmood@tyndall.ie (K.M. Razeeb).

0956-5663/$ – see front matter © 2010 Elsevier B.V. All rights reserved.
doi:10.1016/j.bios.2010.07.071

bilised enzyme is electro active due to the haphazard orientation of enzyme. Thus ordered 3D matrices, such as nanotube arrays (Cui et al., 2007; Lan et al., 2008), ordered porous materials (Zhu et al., 2009) and nanowire, nanorod, nanopillar (Anandan et al., 2006; Gu et al., 2009; Yu et al., 2003) electrode ensembles have been used for increasing the active surface area for enzyme immobilisation. The ordered 3D nanowire arrays with high aspect ratios improve the signal-to-noise ratio significantly, resulting in significantly higher sensitivity and a lower detection limit (De Leo et al., 2007; Xu et al., 2010). Despite the advantage of 3D electrode, nanoparticle modified electrode is getting popular for last couple of years due to their extraordinary catalytic activities (Hrapovic et al., 2004; Karam and Halaoui, 2008; Male et al., 2007; You et al., 2003). Nanoparticles can act as tiny conduction centres and can facilitate the transfer of electrons. Furthermore, it has been reported that enzymes maintained their enzymatic activity when immobilised on nanoparticle modified electrodes.

A number of works have been reported on various strategy of employing GlutOx on to electrode surface to improve the sensitivity (Cooper et al., 1995; Kwon et al., 2005; Kwong et al., 2000; Nakorn et al., 2003; Oldenziel et al., 2004). However, majority of them involved complicated processing steps, which are not efficient to improve the sensitivity, response time and overall reliability of the system. On the other hand, combining nanoparticles with the ordered 3D surface should provide an excellent sensor platform with a larger surface area, which should be able to improve the sensitivity and provide faster response time compared to the reported glutamate sensor. In this work, we fabricated a novel PtNP modified 3D gold NAEs and evaluated them in H_2O_2 detection without using any mediator or enzyme. Biosensor performance of PtNP/NAE was investigated to detect glutamate by immobilising GlutOx on to the surface. To our knowledge, this is the first report on glutamate sensor based on nanoparticle modified ordered 3D array platform.

2. Experimental

2.1. Reagent and materials

Bovine serum albumin (BSA), monosodium glutamate, phosphate buffer saline (PBS) tablets were purchased from Lennox Ireland. Glutamate oxidase (25 units/vial) was purchased from Yamasa Corp., Japan. Nafion (perflurinated ion exchange resin, 5%, w/v) solution and glutaraldehyde (25%, w/v) were purchased from Fluka. The Au electrode bath (PURAMET 402) was purchased from AMI DODUCO. The anodic alumina membrane has a nominal pore size of 200 nm (Whatman Inc.). Potassium hexachloroplatinate and HCl were purchased from Lennox.

2.2. Equipment

Voltammetric and amperometric measurements were performed with a CHI 660C (CH Instruments, Austin, TX) and Versastat 3F (AMETEK PAR, Oak Ridge, TN) (potentiostat/galvanostat). Morphology of modified electrodes was examined using JEOL JSM 6100 scanning electron microscope (SEM). PtNP/NAE was employed as a working electrode with Ag/AgCl and Pt sheet as reference and counter electrode, respectively.

2.3. Procedures

2.3.1. Synthesis of Pt nanoparticle modified-gold nanowire array

Vertically standing gold nanowire arrays were fabricated using a template electrodeposition technique. A thin layer of Au (thickness of 300 nm) was first sputtered onto one side of the AAM template. Electrodeposition of Au was performed at a constant current density of 1.0 mA cm^{-2} for 9000 s in the Au bath (PURAMET 402). After deposition, the AAM template was etched away by submerging the sample in 6.0 M KOH solution for 45 min. The resulting gold NAEs were rinsed in deionised water and punctured to a size of 5 mm diameter of electrode and pasted it to the 3 M transparent gold sputtered polymer film for the electrical connection. Resulting nanowire electrodes were dipped into the Pt solution made of 5 mM potassium hexachloroplatinate and 10 mM HCl and electrodeposition was performed with a current density of 1.0 mA cm^{-2} from 60 to 900 s to fabricate PtNP/NAE.

2.3.2. Enzyme immobilisation

Prior to enzyme immobilisation, PtNP modified NAE was rinsed with acetone and deionised water, followed by running a cyclic voltammetry in 0.5 M H_2SO_4 with a potential range of −0.2 to + 1.5 V at the scan rate of 0.1 V s^{-1} until a stable CV is obtained. 20 μl of GlutOx (25 U in 250 μl of 0.01 M PBS, pH 7.4) was mixed with 2 mg of BSA, 20 μl of glutaraldehyde (2.5%, w/v) and 10 μl of Nafion (0.5%). 10 μl of this mixture was then dispensed onto the surface of a PtNP/NAE and allowed to dry for 60 min under ambient conditions. The electrodes were then stored at 4 °C overnight in 0.01 M PBS buffer prior to use.

Electrode stability was evaluated using amperometry at E_{app} = 0.65 V vs. Ag/AgCl by addition of 200 μM of L-glutamate at room temperature (22 °C). Testing was performed every 3 days for a period of 2 weeks. In between measurement, electrode is stored in PBS at 4 °C.

3. Results and discussion

3.1. Morphology of the NAE and PtNP modified NAEs

Fig. 1 shows SEM images of gold NAE, PtNP modified-gold NAEs and enzyme immobilised PtNP/NAE. The average length of the nanowires is approximately 6 μm with the diameter of ∼200 nm (Fig. 1A). Fig. 1A shows the fabricated nanowires after removing the AAM template. Fig. 1B clearly shows that PtNPs were formed on the nanowire surface after 100 s of deposition at a current density of 5 mA cm^{-2}. With increasing deposition time, more PtNPs were deposited on the nanowire, covers more or less all over the area and concentrated on top of the nanowires like a flower (Fig. 1C). Fig. 1D shows immobilised GlutOx on PtNP/NAE, where homogeneous immobilisation within Nafion polymer layer can be observed. The cross-sectional image (inset of Fig. 1D) shows that the enzyme mixture could cover up to two third of the nanowires' length, which increased the amount of immobilised enzyme within a specific surface area.

3.2. Electrochemical characterisation of PtNP modified NAEs

Fig. 2A illustrates the stepwise fabrication process of the GlutOx/PtNP/NAEs. Fig. 2B shows the cyclic voltammetry of the flat gold electrode (AuE) (circular Au coated polymer with 5 mm diameter) and PtNPs modified flat gold electrode (PtNP/AuE). Fig. 2C shows the same for gold nanowire array electrode (NAE) and PtNPs modified NAEs (PtNP/NAE). All these experiments were performed in 0.5 M H_2SO_4 at a scan rate of 0.1 V s^{-1}. The PtNP/NAE displays typical voltammogram, characteristics of metallic Pt electrode in 0.5 M H_2SO_4 (Fig. S1 of the supplementary information). The electrochemically active surface area of PtNP was determined from the charge consumed during the hydrogen adsorption/desorption (Chakraborty and Retna Raj, 2009). The loading of nanoparticle was optimised on the surface of NAE, where 600–800 s found to be the optimum deposition time (Fig. S2 of the supplementary information) at a current density of 5 mA cm^{-2}. Longer deposition time of PtNP on NAE has negative effect on the active surface area, which may be attributed to the blocking effect by the nanoparticles, due

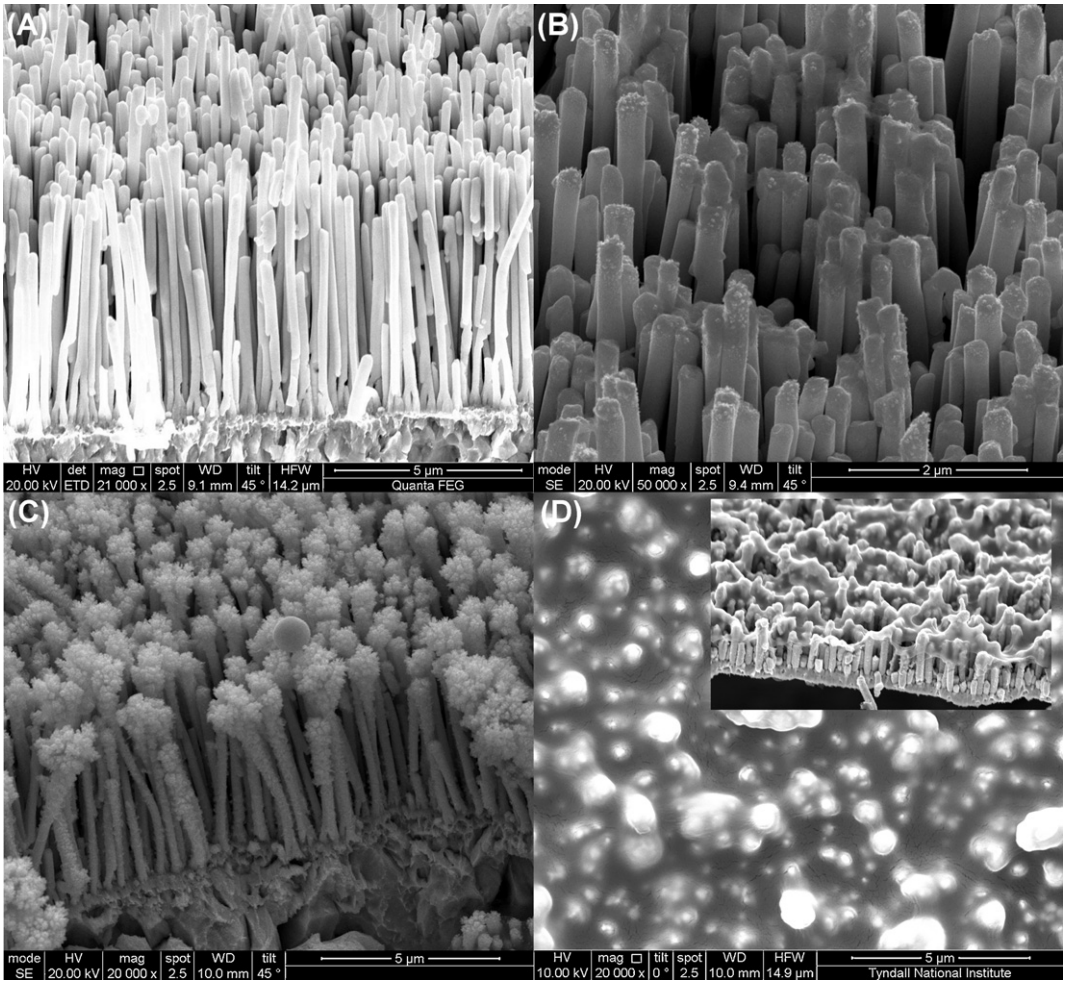

Fig. 1. SEM images of the (A) NAE; (B) 100 s PtNP deposited NAE; (C) 600 s PtNP modified NAE and (D) GlutOx/PtNP/NAE.

to larger amount of deposition at the top of the NAEs as evident from Fig. 1C. Moreover, large amount of PtNP reduce the inter particle distance, which effectively reduce the active surface area (Karam and Halaoui, 2008). Roughness ratio of the flat Au, NAE and PtNP/NAE is calculated by integrating the voltammogram from +0.72 to +1.2 V for flat Au and NAE (Fig. 2B); from +0.20 to +0.80 V for PtNP/AuE and PtNP/NAE (Fig. 2C) electrodes (Xu et al., 2010). Roughness is increased by 26.6 times for NAE electrodes compared to the flat Au electrode and increased by 4.3 times for PtNP/NAE compared to flat Au/PtNP electrode.

3.3. Amperometric behaviour towards H_2O_2

Fig. 3 showed the amperogram of direct electro-oxidation of H_2O_2 on PtNP/NAE electrode at $E_{app} = 0.65$ V vs. Ag/AgCl. To obtain the amperogram, 200 μM of H_2O_2 was added at a regular interval (Fig. 3 inset and also Fig. S4 of the supplementary information for a larger image). Reproducible response was obtained upon repeated addition of H_2O_2, with a sensitivity of 194.6 μA mM^{-1} cm^{-2} at 20 °C and a linear range of up to 20 mM. It confirms that electrode does not undergo deactivation during

Table 1
Analytical performance parameters of AuE, PtNP/AuE, NAE and PtNP/NAE using no enzyme for detection of H_2O_2.

Electrodes	r^2	t_{90} (s)	Linearity (mM)	Detection limit (μM)	Sensitivity (μA mM^{-1} cm^{-2})
AuE	0.9972	55	2.0–20	47	2.35 ± 0.11
PtNP/AuE	0.9627	18	0.02–18	23	166.4 ± 7.9
NAE	0.9628	16	1.0–16	5	8.0 ± 0.38
PtNP/NAE	0.9847	11	0.02–20	1	194.6 ± 9.2

Table 2
A comparison of the performance of some sensor platforms using PtNPs on nano-array electrodes for H_2O_2 detection.

Electrodes	Sensitivity (μA mM^{-1} cm^{-2})	Linear range (mM)	LOD (μM)	References
PtNP/NAE	194.6	0.02–20	1.0	This paper
PtNP–CNT arrays	140	5×10^{-3}–25	1.5	Wen et al. (2009)
PtNP–TiO_2 nanotube arrays	1.68	4×10^{-3}–1.25	4.0	Cui et al. (2008)
PtNP–CNT TiO_2 nanotube arrays	0.134	1×10^{-3}–2	1.0	Pang et al. (2009)
Pt–AuNP TiO_2 nanotube arrays	2.92	10×10^{-3}–80×10^{-3}	10	Kang et al. (2008)

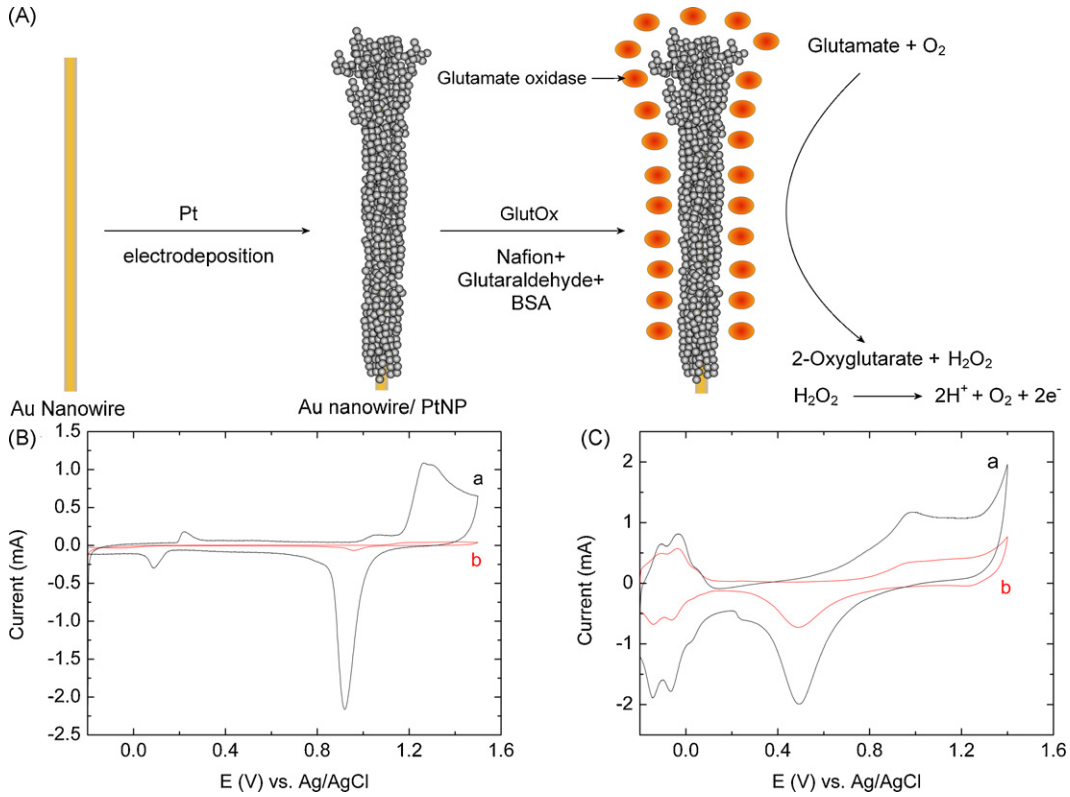

Fig. 2. (A) Schematic illustration of stepwise fabrication of the GlutOx/PtNP/NAEs electrodes. (B) Cyclic voltammograms of the Au NAE (a) and flat Au electrode (b). (C) Cyclic voltammograms of the PtNP/NAE (a) and PtNP on flat Au electrode (b) in 0.5 M H_2SO_4 at 0.1 V s^{-1} (active surface area of blank Au 0.2 cm^2, NAE 1.3 cm^2, PtNP/Au 6.7 cm^2 and PtNP/NAE 10 cm^2, surface areas were calculated using Randles–Sevcik equation using 4 mM Ferricyanide solution).

the experiments. Without using any redox mediator or enzyme, PtNP/NAE can detect H_2O_2 as low as 1 μM at ambient. Moreover, PtNP/NAE showed 24 times higher in sensitivity toward H_2O_2 compared to Au NAE and 82 times compare to flat Au electrode (Fig. S3 of the supplementary information). However, sensitivity of PtNP modified flat Au electrode found to be 166.4 μA mM^{-1} cm^{-2} closer to PtNP/NAE 194.6 μA mM^{-1} cm^{-2}, suggests that nanoparticles play a major role in H_2O_2 oxidation. The intra-electrode relative standard deviation (RSD) was found to be 5.96% ($n = 3$), while inter electrode RSD was 9.45% ($n = 3$) for 200 μM of H_2O_2 additions. The overall superiority of PtNP/NAE compared to other electrode platform prepared in this work is based on sensitivity, detection limit, t_{90} and r^2 value (Table 1).

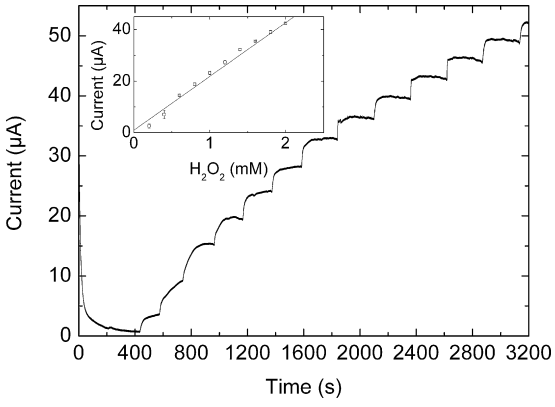

Fig. 3. Amperometric response of PtNP/NAE electrode for successive addition of 0.2 mM H_2O_2 (E_{app} = 0.65 V vs. Ag/AgCl) and corresponding concentration plot (inset). Background electrolyte is 0.01 M PBS (pH 7.4).

A comparison of the performance of some efficient sensor platforms using PtNPs on nano-array electrodes for H_2O_2 detection are presented in Table 2. It can be seen that the proposed PtNP/NAE sensor template shows a good performance in terms of sensitivity, linear range and limit of detection (LOD). However, the calculated sensitivity for all the electrodes in Table 1 was determined by considering a surface area of 0.2 cm^2.

3.4. Analytical performance of the glutamate biosensor

The analytical performance of the PtNP/NAE platform was examined to detect glutamate. GlutOx was achieved by cross-linking with glutaraldehyde (1%, v/v) and BSA (2%, w/v) onto the surface of PtNP/NAEs. The optimum enzyme loading was determined by examining the activity levels over the range of 0.02–0.8 U/electrode glutamate oxidase. An enzyme loading of 0.58 U GlutOx per electrode was found to be optimal where higher loadings resulted in poor substrate response. On the other hand, lower enzyme loadings resulting in poor response sensitivity. To obtain the best cross-linking, the ratio of Nafion, glutaraldehyde and BSA were used following the article published by Jamal et al. (2009).

The potential of the GlutOx immobilised electrode was held at 0.65 V and aliquots of glutamate was injected into oxygen saturated PBS at a regular intervals (Fig. 4). This electrode could successfully detect enzymatically generated H_2O_2. The sensitivity of the electrode towards glutamate obtained from the calibration plot was 10.76 μA mM^{-1} cm^{-2}, which is higher than a large number of reported glutamate oxidase based sensor (Cooper et al., 1995; Jamal et al., 2009; Kwon et al., 2005; Kwong et al., 2000; Nakorn et al., 2003; Oldenziel et al., 2004), where the sensitivity varies between 0.001 and 1.43 μA mM^{-1} cm^{-2}. This would be attributed to the uniform distribution of nanoparticle and a higher amount of

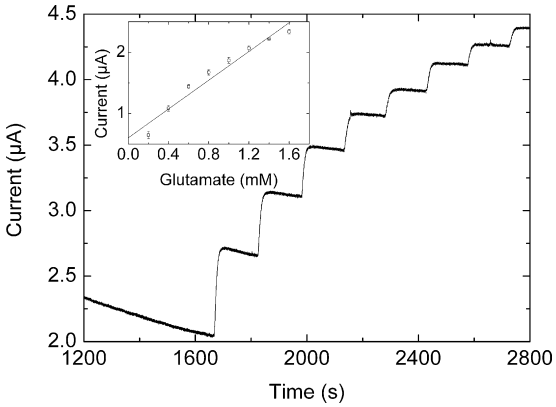

Fig. 4. Amperometric response of GlutOx modified PtNP/NAE electrode for successive addition of 0.2 mM glutamate (E_{app} = 0.65 V vs. Ag/AgCl) and corresponding concentration plot (inset). Background electrolyte is 0.01 M PBS (pH 7.4).

enzyme deposited onto the ordered 3D NAE surface. Fig. 4 (inset) (Fig. S5 of the supplementary information for a larger image) also shows that the GlutOx sensor is linear up to 0.8 mM and starts attaining to a saturation level at higher concentrations as expected by Michaelis–Menten type enzyme kinetics. The limit of detection was found to be 14 μM with t_{90} of 4.6 s, where t_{90} suggests that the electrode responds rapidly to the change of the analyte concentration compared to the reported work. The intra-electrode RSD was found to be 3.23% (n = 3), while inter electrode RSD was 6.65% (n = 3) for 200 μM of glutamate additions.

The stability of the GlutOx modified PtNP/NAEs was determined over a period of 2 weeks, with a analysis carried out every 3 days, 6 assay each day with 200 μM glutamate addition. In between the testing, the electrode is stored in 0.01 M PBS at 4 °C. The enzyme modified electrode was found to retain 98% of its initial activity after 2 weeks, which compared well with Chang et al., 2007 (approximately 100% after 2 weeks).

4. Conclusion

In this article, we have reported a novel platform based on PtNP modified 3D gold nanowire array electrode to detect H_2O_2 without using any mediator or enzyme. PtNP/NAE modified electrode showed 24 times higher in sensitivity toward H_2O_2 compared to Au NAE electrode and 82 times compared to flat Au electrode. This electrode platform is applied successfully to detect glutamate by immobilising GlutOx using cross-linking method, where 14 μM of glutamate can be detected without using any mediator. Moreover, fast response time (<5 s) with high sensitivity towards glutamate (10.76 μA mM^{-1} cm^{-2}) was obtained with a linear range up to 0.8 mM. Glutamate sensitivity found to be higher compare to a large number of reported glutamate oxidase based sensor, where the sensitivity varied between 0.001 and 1.43 μA mM^{-1} cm^{-2}. Further work will extend the system enabling to determine glutamate in real sample.

Acknowledgments

This work was financially supported by Enterprise Ireland (EI) under the commercialisation fund and technology development program, CFTD/2008/322. Helene Rodde is acknowledged for some of the electrochemical measurements.

Appendix A. Supplementary data

Supplementary data associated with this article can be found, in the online version, at doi:10.1016/j.bios.2010.07.071.

References

Anandan, V., Rao, Y.L., Zhang, G.G., 2006. Int. J. Nanomed. 1, 73–79.
Chakraborty, S., Retna Raj, C., 2009. Biosens. Bioelectron. 24, 3264–3268.
Chapman, J., Zhou, M., 1999. Anal. Chim. Acta 402, 47–52.
Cooper, J.M., Foreman, P.L., Glidle, A., Ling, T.W., Pritchard, D.J., 1995. J. Electroanal. Chem. 388, 143–149.
Cui, H.F., Ye, J.S., Zhang, W.D., Li, C.M., Luong, J.H.T., Sheu, F.S., 2007. Anal. Chim. Acta 594, 175–183.
Cui, X.L., Li, Z.Z., Yang, Y.C., Zhang, W., Wang, Q.F., 2008. Electroanal 20, 970–975.
De Leo, M., Kuhn, A., Ugo, P., 2007. Electroanalysis 19, 227–236.
Fonnum, F., 1984. J. Neurochem. 42, 1.
Gu, B.X., Xu, C.X., Zhu, G.P., Liu, S.Q., Chen, L.Y., Wang, M.L., Zhu, J.J., 2009. J. Phys. Chem. B 113, 6553–6557.
Hrapovic, S., Liu, Y.L., Male, K.B., Luong, J.H.T., 2004. Anal. Chem. 76, 1083–1088.
Jamal, M., Worsfold, O., Mccormac, T., Dempsey, E., 2009. Biosens. Bioelectron. 24, 2926–2930.
Kang, Q., Yang, L.X., Cai, Q.Y., 2008. Bioelectrochemistry 74, 62–65.
Karam, P., Halaoui, L.I., 2008. Anal. Chem. 80, 5441–5448.
Kwon, N.H., Won, M.S., Choe, E.S., Shim, Y.B., 2005. Anal. Chem. 77, 4854–4860.
Kwong, A.W.K., Grundig, B., Hu, J., Renneberg, R., 2000. Biotechnol. Lett. 22, 267–272.
Lan, D., Li, B.X., Zhang, Z.J., 2008. Biosens. Bioelectron. 24, 934–938.
Male, K.B., Hrapovic, S., Luong, J.H.T., 2007. Analyst 132, 1254–1261.
Martin, S.J., Grimwood, P.D., Morris, R.G.M., 2000. Annu. Rev. Neurosci. 23, 649–711.
Nakorn, P.N., Suphantharika, M., Udomsopagit, S., Surareungchai, W., 2003. World J. Microbiol. Biotechnol. 19, 479–485.
Oldenziel, W.H., Beukema, W., Westerink, B.H.C., 2004. J. Neurosci. Methods 140, 117–126.
Olney, J.W., Farber, N.B., 1995. Arch. Gen. Psychiatry 52, 998–1007.
Pang, X.Y., He, D.M., Luo, S.L., Cai, Q.Y., 2009. Sens. Actuators B 137, 134–138.
Rietz, B., Guilbault, G.G., 1975. Anal. Chim. Acta 77, 191–198.
Swanepoel, E., De Villiers, M.M., Du Preez, J.L., 1996. J. Chromatogr. A 729, 287–291.
Symthies, J., 1999. Eur. J. Pharmacol. 370, 1–7.
Tucci, S., Pinto, C., Goyo, J., Rada, P., Hernández, L., 1998. Clin. Biochem. 31, 143–150.
Umar, A., Rahman, M.M., Kim, S.H., Hahn, Y.B., 2008. Chem. Commun., 166–188.
Valero, E., Garcia-Carmona, F., 1998. Anal. Biochem. 259, 265–271.
Wen, Z.H., Ci, S.Q., Li, J.H., 2009. J. Phys. Chem. C 113, 13482–13487.
Xu, J., Shang, F., Luong, J.H.T., Razeeb, K.M., Glennon, J.D., 2010. Biosens. Bioelectron. 25, 1313–1318.
Yang, M.H., Yang, Y.H., Liu, Y.L., Shen, G.L., Yu, R.Q., 2006. Biosens. Bioelectron. 21, 1125–1131.
You, C.P., Li, X., Zhang, S., Kong, J.L., Zhao, D.Y., Liu, B.H., 2009. Microchim. Acta 167, 109–116.
You, T.Y., Niwa, O., Tomita, M., Hirono, S., 2003. Anal. Chem. 75, 2080–2085.
Yu, S.F., Li, N.C., Wharton, J., Martin, C.R., 2003. Nano Lett. 3, 815–818.
Zhu, Y.H., Cao, H.M., Tang, L.H., Yang, X.L., Li, C.Z., 2009. Electrochim. Acta 54, 2823–2827.